

RESEARCH

Open Access



Epimedin B protects against bone loss and inflammation in diabetic osteoporosis rats by regulating OPG/RANKL pathway

Xianmei Zhang¹, Qinguo Sun¹, Xie Xie¹, Meng Luo¹, Junjie Zan¹ and Zewei Cong^{1*}

Abstract

Background Diabetes is a common disease contributing to osteoporosis. Epimedin B (EB), a major ingredient of *Herba Epimedii*, has been found to be effective in preventing osteoporosis in mice. However, the potential of EB to ameliorate diabetic osteoporosis (DOP) remains elusive. In this study, our goal is to investigate the functions and underlying mechanisms of EB in the progression of DOP.

Methods A DOP rat model was established via a high-fat diet combined with intraperitoneal injection of streptozotocin (STZ). DOP rats were daily administered with EB or vehicle via intragastric administration for 8 weeks. Body weights and blood glucose levels were measured every 4 weeks during the drug administration period. Blood samples and femoral tissues were collected for further analysis. Bone parameters and bone histopathological changes were detected. Bone formation and resorption markers as well as inflammatory factors were detected using enzyme-linked immunosorbent assay kits. Reverse-transcription quantitative polymerase chain reaction and western blotting were conducted to measure the expression of osteoprotegerin (OPG) and Rev-Erba, receptor activator of NF- κ B ligand (RANKL).

Results EB improved weight loss and lowered blood glucose of DOP rats. EB promoted the formation of bone trabeculae and altered several bone microstructure parameters in DOP rats. EB ameliorated improved bone structure, restored histological abnormalities of femoral bone, and reduced the number of bone marrow adipocytes in DOP rats. EB inhibited excessive bone resorption and inflammation and increased bone formation in DOP rats. EB regulated the OPG/RANKL axis in DOP rats.

Conclusion EB attenuates STZ-induced DOP in rats by maintaining the balance between bone formation and resorption and inhibiting inflammation through regulating the OPG/RANKL axis.

Keywords Diabetes, Osteoporosis, Epimedin B, Bone formation, Bone resorption, Inflammation, OPG/RANKL axis

*Correspondence:

Zewei Cong

Zeweicongdoc@hotmail.com

¹Department of Traditional Chinese Medicine, Wuhan Third Hospital, Wuhan 430000, China



© The Author(s) 2025. **Open Access** This article is licensed under a Creative Commons Attribution-NonCommercial-NoDerivatives 4.0 International License, which permits any non-commercial use, sharing, distribution and reproduction in any medium or format, as long as you give appropriate credit to the original author(s) and the source, provide a link to the Creative Commons licence, and indicate if you modified the licensed material. You do not have permission under this licence to share adapted material derived from this article or parts of it. The images or other third party material in this article are included in the article's Creative Commons licence, unless indicated otherwise in a credit line to the material. If material is not included in the article's Creative Commons licence and your intended use is not permitted by statutory regulation or exceeds the permitted use, you will need to obtain permission directly from the copyright holder. To view a copy of this licence, visit <http://creativecommons.org/licenses/by-nc-nd/4.0/>.

Introduction

Diabetes is a chronic medical condition characterized by persistent hyperglycemia, and both type 1 and type 2 diabetes affect millions of individuals worldwide. Type 2 diabetes is much more prevalent than type 1 diabetic mellitus, representing 90% of diabetes cases globally. According to estimates in 2021, the global diabetes prevalence in 20–79 years old was approximately 10.5% (536.6 million people), a figure projected to rise to 12.2% (783.2 million) by 2045. The diabetes prevalence of Chinese adults aged 20–79 years accounts for over a quarter of the global diabetes population [1]. Osteoporosis is a metabolic bone disease characterized by a systemic impairment of bone mass and microarchitecture that results in fragility fractures. Type 2 diabetes is recognized as an important osteoporosis risk factor. It can affect bone health, resulting in decreased bone formation, increased bone marrow adiposity, and heightened risk of fracture [2]. Patients with type 2 diabetes are at increased risk for osteoporosis than those without diabetes [3]. The prevalence of osteoporosis in patients with type 2 diabetes are 27.67% worldwide and 35.77% in China [4, 5]. With the increasing prevalence of diabetes, the burden of diabetes-induced osteoporosis (DOP) is increasing worldwide. Currently, DOP is often treated with antiresorptive therapies (such as bisphosphonate and denosumab) or anabolic drugs (such as teriparatide and abaloparatide) [6–9]. However, their long-term adverse reactions such as atypical fracture, muscle and joint pain, and increased risk of stroke restrict their clinical application [10]. Therefore, it is urgent to continue developing drugs for prevention and treatment of DOP.

Bone remodeling is a highly regulated, lifelong process of bone resorption and formation [11]. When bone resorption and formation are imbalanced, bone remodeling cycle may be highly altered, leading to metabolic bone disease, most commonly osteoporosis [12]. Osteoblasts are specialized mesenchymal cells that can differentiate into chondrocytes and adipocytes. Mature osteoblasts synthesize bone matrix proteins such as osteopontin, osteocalcin (OCN), and osteonectin and are rich in alkaline phosphatase (ALP) [13, 14]. Additionally, osteoblasts secrete osteoprotegerin (OPG) and can inhibit differentiation and function of osteoclasts by binding to receptor activator of nuclear κ B ligand (RANKL), preventing RANKL from binding to RANK. The ratio of OPG/RANKL is an important determinant of bone mass and skeletal integrity [15].

Traditional Chinese medicine (TCM) has been widely used in China and shows unique advantages in the treatment of osteoporosis [16]. Many natural compounds have attracted increasing attention as anti-osteoporosis drugs, such as luteoloside [17], aliseol-B [18], andrographolide [19], matairesinol [20], and quercetin [21].

Therefore, natural compounds may be a promising treatment scheme for osteoporosis disease. Epimedii Herba is a classic TCM with proven efficacy in treating cardiovascular diseases and osteoporosis [22]. Epimedin B (EB) is the second highest active ingredient in the flavonoids of Herba Epimedi. A previous study has suggested that EB is effective in treating osteoporosis in mice through PI3K/AKT, MAPK, and PPAR pathways [23]. In diabetes mellitus, hyperglycemia is a condition that promotes the release of inflammatory mediators, and inflammatory mediators are elevated in diabetic patients compared with nondiabetic subjects [24]. Inflammation and hyperglycemia caused by diabetes can induce apoptosis of mature osteoblasts [25]. It is found that proinflammatory cytokines and chemokines are associated with osteoclastic bone loss, and they function by promoting RANKL production and reducing OPG production [26]. The anti-inflammatory property of EB has been previously established [27]. However, current evidence is limited to confirm the protective effect of EB against DOP.

In this study, our goal is to investigate the functions and underlying mechanisms of EB in the progression of DOP. We hypothesize that EB may prevent the progression of DOP. To test this hypothesis, we construct a streptozotocin (STZ)-induced DOP model in rats. Our findings may provide insights into the pharmacological properties of EB concerning the progression of DOP.

Methods

Ethical statement

All animal experiments were reviewed and approved by Wuhan Myhalic Biotechnology Co., Ltd (approval number: HLK-202309244; approval date: September 15, 2023) and performed following the guidelines of the National Institutes of Health Guide for the Care and Use of Laboratory Animals.

Animals

Fifty male Sprague-Dawley (SD) rats (180–230 g; Charles River Laboratories, Beijing, China) were housed in a specific-pathogen-free animal room with standard conditions ($24 \pm 2^\circ\text{C}$, 60–80% of humidity, and a 12-h light/dark cycle) and with free access to food and water. Five rats were kept in one cage. After adaptive feeding for a week, fifty rats were randomized into two groups: 10 rats in the control group were fed with a normal diet (energy composition, 15.8% fat, 20% protein, and 63.9% carbohydrate) and 40 rats in the high-fat group were fed with a high-fat diet (energy composition, 45% fat, 20% protein, and 35% carbohydrate) for 4 weeks. Then, the rats fed with a high-fat diet were intraperitoneally injected with 1% streptozotocin (STZ; MedChemExpress, Shanghai, China) at 30 mg/kg daily for 5 days [28]. Three days later after STZ injection, the rats were fasted for an additional

8 h (water was allowed), and tail venous blood was harvested to measure fasting blood glucose (FBG). Rats with FBG levels ≥ 16.7 mmol/L were considered as successfully established type 2 diabetic rats [29]. To induce osteoporosis, type 2 diabetic rats were maintained on a high-fat diet for an additional 8 weeks.

After that, diabetic rats were randomized into four groups ($n=10$): DOP model (DOP) group, DOP with 10 mg/kg EB (DOP+EB-10) group, DOP with 20 mg/kg EB (DOP+EB-20) group, and DOP with 40 mg/kg EB (DOP+EB-40) group. Each group had 10 rats. The rats in Control and DOP groups were both administered with 10% Tween 80 and 90% sterile water (vehicle control) through intragastric administration for 8 weeks. The rats in DOP+EB-10, DOP+EB-20, and DOP+EB-40 groups were daily administered with 10 mg/kg, 20 mg/kg, and 40 mg/kg EB (purity 99.81, MedChemExpress) through intragastric administration, respectively, for 8 weeks. The dosages of EB were determined based on previous studies [23, 30]. Body weights and blood glucose levels were measured every four weeks over the course of EB treatment. After the last administration of EB or vehicle, all rats were fasting for 8 h and sacrificed by cervical dislocation under 4% isoflurane anesthesia. Blood samples were harvested by heart puncture via exsanguination for enzyme-linked immunosorbent assay (ELISA) assays. Bilateral femurs were immediately harvested and fixed in 4% paraformaldehyde for histological staining or stored at -80°C for further analysis.

Micro-CT analysis

Femoral samples were precisely positioned within the scanning area and underwent Micro-CT (SkyScan1176, Bruker, Germany) scanning with a $9\ \mu\text{m}$ voxel. The images were acquired at 80 Kv voltage and 88 μA current. Then, osteoporosis-related parameters within a defined region of interest were calculated using Airbone software, including bone mineral density (BMD), bone volume fraction (BV/TV), trabecular separation (Tb.Sp), and trabecular number (Tb.N).

Biomechanical testing of femur maximum load

After removal of muscles and soft tissues, the femurs were air-dried and secured onto a three-point bending jig with a 20 mm span. A universal mechanical testing machine applied compression at a rate of 1 mm/min until a complete bone fracture, and the maximum load was recorded.

Histopathological changes

Femoral samples were fixed with 10% neutral-buffered formalin (Sigma-Aldrich, Shanghai, China) for 48 h and then immersed in 10% EDTA solution (MedChemExpress) for a month. Subsequently, femur sections were

embedded in paraffin wax and sectioned into $4\ \mu\text{m}$ thick slices. Thereafter, tissue sections were deparaffinized and rehydrated, followed by 10 min of hematoxylin and 5 min of eosin staining (Sigma-Aldrich) for histopathological examination. The number of adipocytes (adipocytes/ mm^2) was counted using Image Pro Plus software.

ELISA

Blood samples were centrifuged at 3000 rpm for 10 min at 4°C , and serum was separated and stored at -80°C . OCN, bone alkaline phosphatase (BAP), tartrate-resistant acid phosphatase 5b (TRACP-5b), tumor necrosis factor (TNF)- α , interleukin (IL)-6, and monocyte chemoattractant protein-1 (MCP-1) in rat serum were detected using commercially available ELISA kits (Nanjing Jiancheng Bioengineering institute, Nanjing, China) according to the manufacturer's instructions. Briefly, 100 μL serum samples were added to the microplate and incubated for 2 h. Then, equal volumes of primary antibodies against OCN, BAP, TRACP-5b, TNF- α , IL-6, and MCP-1 were added to each well and incubated for another 1 h, followed by incubation with horseradish-peroxidase (HRP)-conjugated secondary antibodies for 30 min. All the above incubations were performed at 37°C , washing 3 times with Tris Buffered Saline Tween 20 (TBST) after each incubation. The optical density values at 450 nm were detected using a microplate reader (Thermo Fisher, Shanghai, China). The concentrations of OCN, BAP, TRACP-5b, TNF- α , IL-6, and MCP-1 in the serum samples were proportional to the optical density values.

Reverse-transcription quantitative polymerase chain reaction (RT-qPCR)

Total RNA was isolated from 20 mg femoral samples using TRIzol reagent (Beyotime, Shanghai, China) following the manufacturer's instructions. Using a NanoDrop spectrophotometer (Thermo Fisher), total RNA concentration was evaluated by detecting absorbance at 260 nm. Then, total RNA (1 μg) was reverse transcribed into cDNA using a Prime Script RT Reagent Kit (Takara, Tokyo, Japan). Next, RT-qPCR was performed using ABI Prism 7500 (Applied Biosystems, Waltham, MA, USA) with SYBR Green RT-qPCR Master Mix (Applied Biosystems). The thermocycling conditions were 95°C for 10 min and then 40 cycles of 95°C for 20 s and 60°C for 30 s. A melting curve was acquired using 95°C for 15 s, 60°C for 30 s, and 95°C for 15 s. Relative mRNA expressions were calculated using the $2^{-\Delta\Delta\text{Ct}}$ method and normalized to GAPDH expression. The primers used in this study were listed as follows: OPG, forward 5'-GGCAGG GCATACTTCCTGTT-3', reverse 5'-GCCACTTGTTCA TTGTGGTCC-3'; RANKL, forward 5'-AGGCTGGGCC AAGATCTCTA-3', reverse 5'-GATAGTCCGCAGGTAC

GCTC-3'; GAPDH, forward 5'-CCACCCATGGCAAAT TCCATGGCA-3', reverse 5'-TCTAGACGGCAGGTCA GGTCCACC-3'.

Western blotting

Protein extraction from 20 mg femoral samples was accomplished using 200 μ L of RIPA lysis buffer (Beyotime, Shanghai, China) supplemented with 1% phenylmethylsulfonyl fluoride (PMSF; Beyotime) and protease inhibitor cocktail (Beyotime). Then, equal amounts (40 μ g/lane) were separated by electrophoresis on 10% sodium dodecyl sulfate-polyacrylamide gel electrophoresis gels and transferred onto polyvinylidene difluoride membranes. Subsequently, the membranes were blocked with 5% skimmed milk for 1 h at room temperature and incubated with primary antibodies against OPG (ab73400, 1:5000; Abcam, Shanghai, China), RANKL (sc-59982, 1:1000; Santa Cruz Biotechnology, Shanghai, China), and β -actin (ab8226, 1:1000; Abcam) overnight at 4°C. On the next day, the membranes were washed with TBST three times and incubated with corresponding horseradish peroxidase-conjugated secondary antibodies at room temperature for 1 h. Finally, the membranes were washed three times in TBST and monitored with an enhanced chemiluminescence reagent (Thermo

Fisher, Shanghai, China) and visualized on Odyssey Infrared Imaging system (Li-Cor Bioscience, Lincoln, NE, USA). Protein expression was measured by analyzing the intensities of the protein bands with ImageJ software. The intensity values were normalized to that of β -actin.

Statistical analysis

Data was obtained from at least three independent experiments by two pathologists who were blinded to study design. Statistical analysis was analyzed using GraphPad Prism 8 (GraphPad Software, San Diego, CA, USA) and described as the mean \pm standard deviation. One-way analysis of variance followed by Tukey's post *hoc* analysis was used for comparison analyses. $p < 0.05$ was considered statistically significant.

Results

EB improves weight loss and blood glucose of DOP rats

First, we detected the effect of EB on rat body weights and blood glucose levels. The chemical structure of EB was shown in Fig. 1A. The results revealed that compared with normal rats, STZ-induced DOP rats had significantly lower body weights and higher fasting blood glucose concentrations. However, treatment with EB (10, 20, and 40 mg/kg) for 8 weeks significantly reversed these

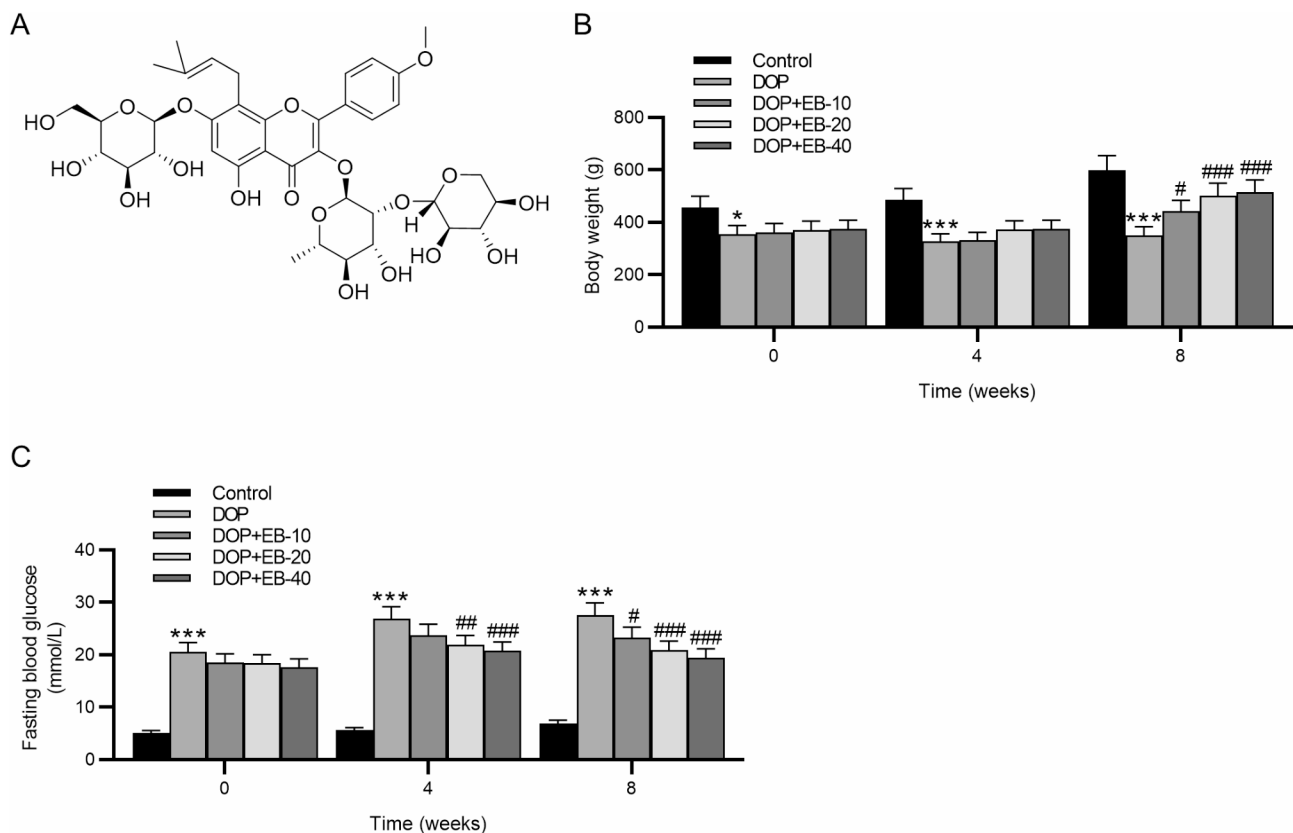


Fig. 1 EP improves weight loss and blood glucose of DOP rats. **(A)** Chemical structure of Epimedin B (EB). **(B)** Change in body weights. **(C)** Change in blood glucose concentrations. * $p < 0.05$, *** $p < 0.001$ vs. Control group; # $p < 0.05$, ## $p < 0.01$, ### $p < 0.001$ vs. DOP group

outcomes (Fig. 1B-C). These results show that 8 weeks of EB treatment at 10, 20, and 40 mg/kg effectively improves STZ-induced weight loss and hyperglycemia in DOP rats.

EB prevents bone mass loss in DOP rats

Then, we examined the effect of EB on bone microstructure. In the DOP group, micro-CT scans revealed sparse trabecular structure and significant bone mass loss in the femurs. However, EB treatment suppressed bone mass loss in the femurs of DOP rats dose-dependently (Fig. 2A). We also quantified BMD and trabecular micro-architectural parameters including BV/TV, Tb.Sp, and Tb.N. BMD is an index reflecting alterations in bone mass and bone strength. BV/TV reflects the value of bone volume and serves as a significant index for evaluating the alteration of bone mass. Tb.Sp is the average width of the medullary cavity between bone trabeculae, reflecting the morphology and structure of bone trabeculae. Tb.N is the number of intersections between bone tissue and non-bone tissue and reflects the morphological structure of bone trabeculae and the ratio of bone area to bone mass, explaining the changer in bone mass [31]. Compared with normal rats, DOP rats had notably decreased BMD, BV/TV, and Tb.N and substantially increased Tb.Sp. However, 8 weeks of EB treatment (10 and 20 mg/kg) markedly reversed these changes in DOP rats in a dose-dependent manner (Fig. 2B-E). Additionally, the

bone biomechanical properties were assessed by three-point bending tests, and the results revealed that the maximum load borne by DOP rat femurs was remarkably reduced compared with normal rat femurs, which was remarkably enhanced by EB (10 and 20 mg/kg) dose-dependently (Fig. 2F). These results show that EB attenuates bone mass loss in DOP rats.

EB ameliorates histological abnormalities of femoral bone in DOP rats

Next, histological staining was performed on distal femurs and bone marrow cavities. As hematoxylin and eosin staining revealed, normal rats exhibited abundant, dense, moderately thick, and well-orderedly distributed femoral trabecular bone as well as sparsely distributed bone marrow adipocytes with low density. However, the trabecular bone became thinner and disorganized, and the trabecular separation increased, along with the marrow adipocyte density and volume were enhanced in DOP rats. Conversely, EB treatment greatly improved trabecular structure, promoted new bone formation, and inhibited marrow adipogenesis in a dose-dependent manner (Fig. 3A-C). These results show that EB significantly improves bone microstructure and inhibits marrow adipogenesis in DOP rats.

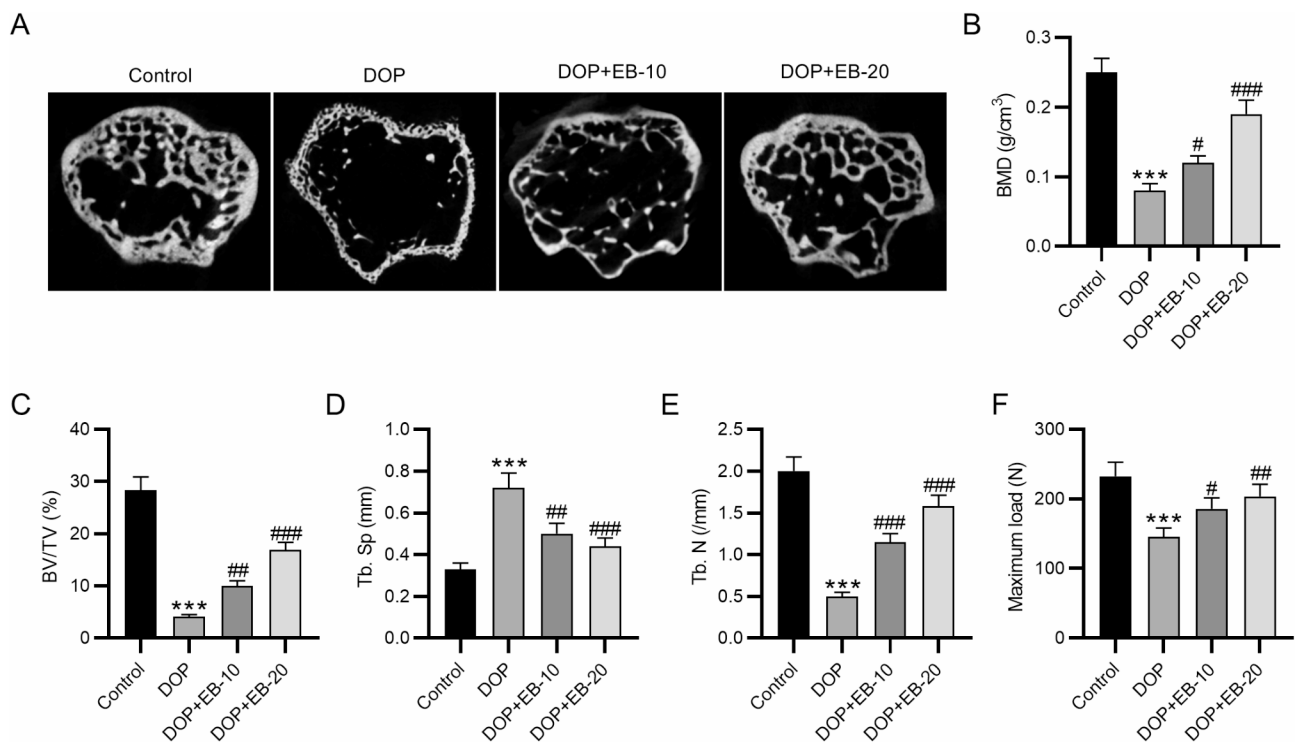


Fig. 2 EB prevents bone loss in DOP rats. **(A)** Three-dimensional images of bone trabecula. **(B)** Bone mineral density (BMD). **(C)** Relative bone volume over total volume (BV/TV). **(D)** Trabecular separation (Tb.Sp). **(E)** Trabecular number (Tb.N). **(F)** Maximum load for the proximal femur. *** $p < 0.001$ vs. Control group; # $p < 0.05$, ## $p < 0.01$, ### $p < 0.001$ vs. DOP group

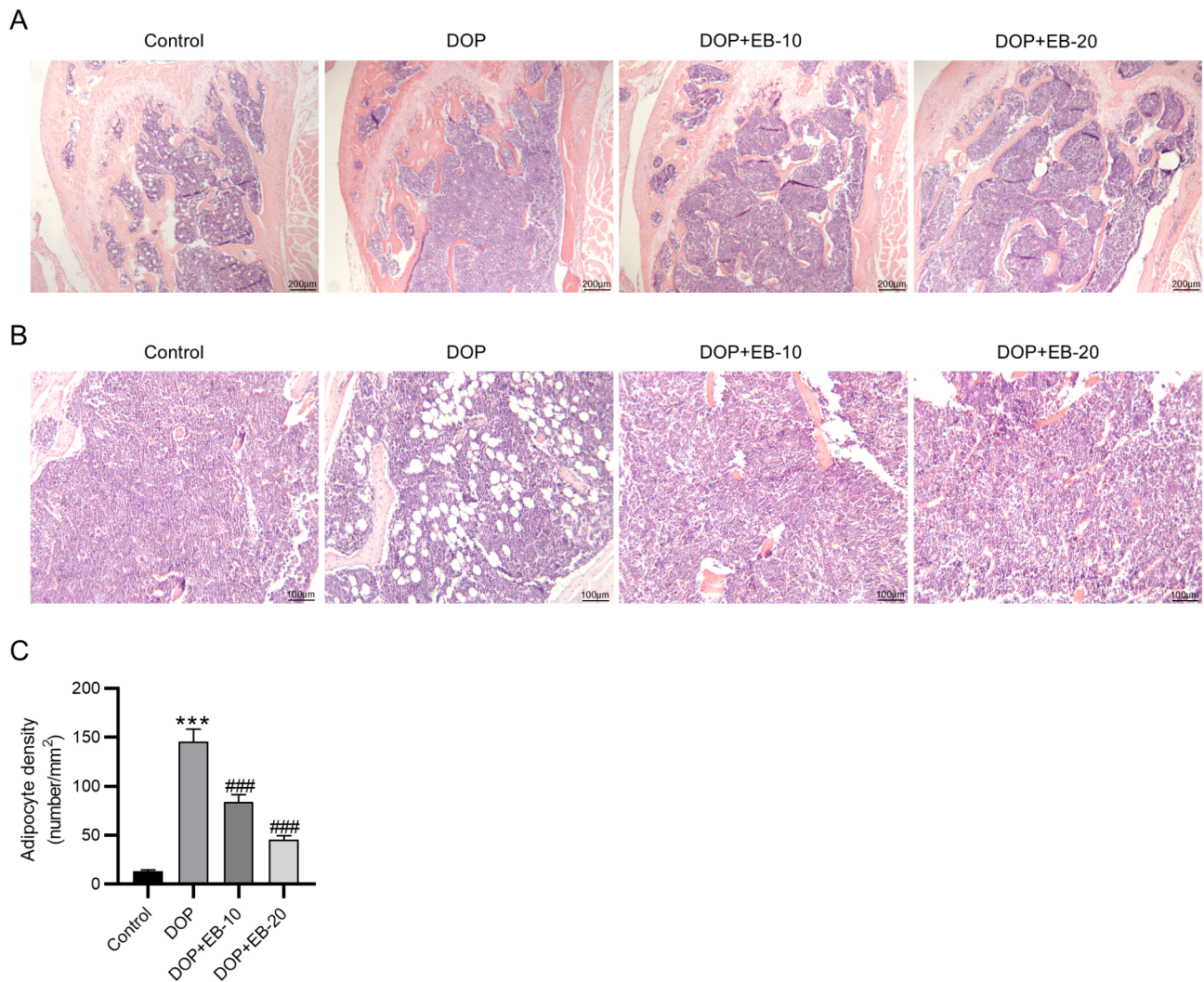


Fig. 3 EB ameliorates histological abnormalities of femoral bone in DOP rats. **(A)** Representative hematoxylin-eosin staining of femur sections. **(B)** Representative hematoxylin-eosin staining of bone marrow adipocytes. **(C)** Quantification of the number of adipocytes per square millimeter. *** $p < 0.001$ vs. Control group; ### $p < 0.001$ vs. DOP group

EB inhibits bone turnover and inflammation in DOP rats

Moreover, we assessed the serum levels of OCN, BAP, and TRACP-5b, which could be used to evaluate osteoblastic and osteoclastic activities. It was found that the DOP group exhibited markedly lower OCN and BAP levels and higher TRACP-5b level in serum than the control group, whereas EB treatment reversed the effect of STZ on decreasing OCN and BAP levels and increasing TRACP-5b level in serum of DOP rats (Fig. 4A-C). Meanwhile, the STZ-induced significant elevation in the serum levels of IL-6, TNF- α , and MCP-1 in DOP rats was dose-dependently abolished by EB (Fig. 4C-E). These results indicate that EB inhibits bone turnover and inflammation in DOP rats.

EB regulates the OPG/RANKL axis in DOP rats

Finally, we detected the underlying mechanisms responsible for the protective effect of EB against DOP. As RT-qPCR and western blotting demonstrated, the DOP group had lower OPG and higher RANKL mRNA and protein levels than the control group, whereas EB treatment had the opposite effect (Fig. 5A-D). These results indicate that EB might exert protective effects against DOP through regulating the OPG/RANKL axis.

Discussion

Diabetes is a pandemic health problem, and its incidence is constantly increasing. Emerging evidence has suggested that diabetes poses a risk for osteoporosis and can contribute to the development of DOP [32–34]. In diabetes patients, approximately 50–60% show a decreasing trend in bone mineral density, and approximately 33% are

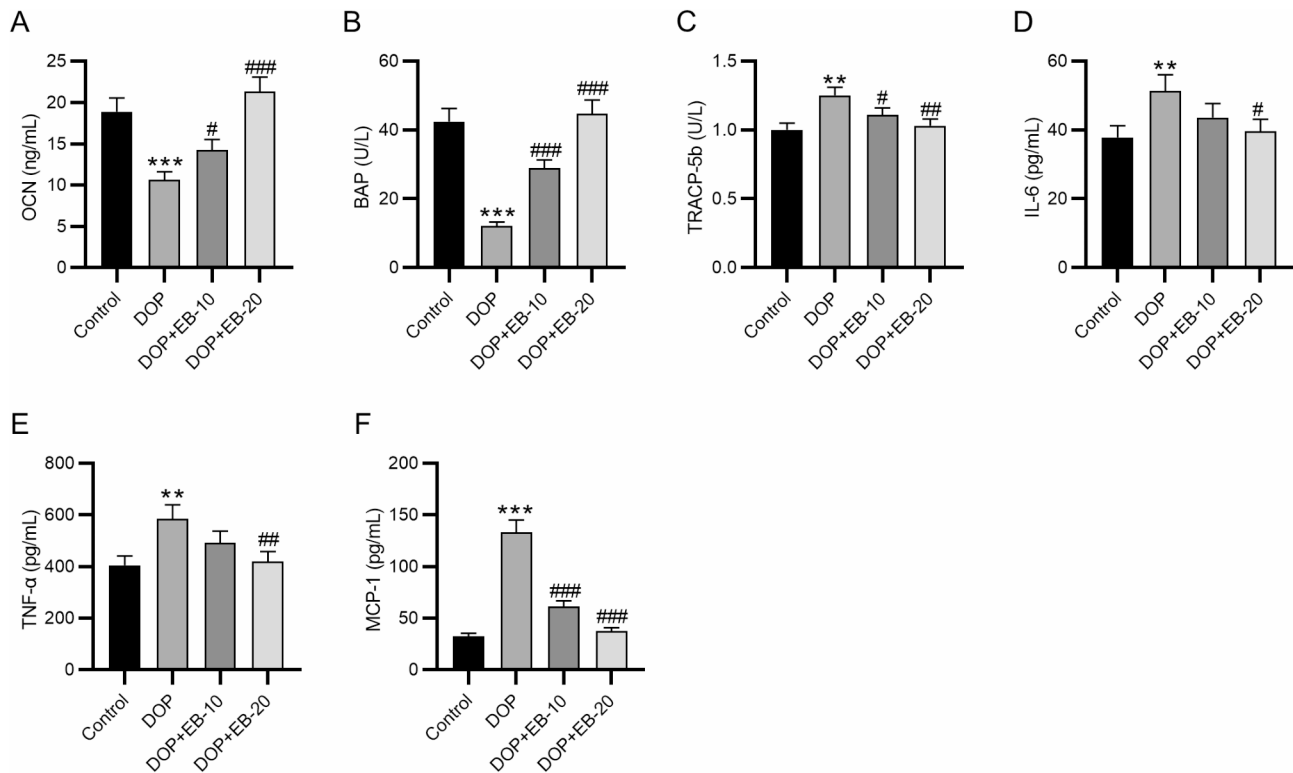


Fig. 4 EB inhibits bone turnover and inflammation in DOP rats. **(A)** ELISA of osteocalcin (OCN) level in the serum. **(B)** ELISA of bone alkaline phosphatase level in the serum. **(C)** ELISA of tartrate-resistant acid phosphatase-5b (TRACP-5b) level in the serum. **(D)** ELISA of IL-6 level in the serum. **(E)** ELISA of TNF- α level in the serum. **(F)** ELISA of MCP-1 level in the serum. ** $p < 0.01$, *** $p < 0.001$ vs. Control group; # $p < 0.05$, ## $p < 0.01$, ### $p < 0.001$ vs. DOP group

diagnosed with osteoporosis [35]. TCM, with few side effects, has unique advantages in the treatment of osteoporosis [36]. Herba Epimedii, also known as YinYangHuo in Chinese, is a Chinese herbal medicine and has been used in combination with other herbs to treat skeletal diseases in TCM [37]. EB, a major ingredient of Herba Epimedii, has been found to be effective in preventing osteoporosis in vitro and in mice and has an anti-inflammatory effect [23, 27]. However, the role and regulatory mechanism of EB in DOP remain elusive. In this study, we constructed an STZ-induced DOP rat model that shows a significant increase in hyperglycemia, weight loss, bone mass loss, and bone microarchitecture deterioration. Our findings revealed that EB may be a potential candidate for the treatment of DOP.

Bone remodeling is an essential process for preserving bone integrity and mineral homeostasis. During the bone remodeling cycle, osteoclastic resorption is tightly coupled to osteoblastic bone formation. However, this balance is disrupted in osteoporosis patients [38]. Osteoblasts, bone forming cells, arise from the commitment of mesenchymal precursors to osteoprogenitor lineages and can produce extracellular proteins, including OCN, ALP, and type I collagen [38]. Osteoclasts, bone-resorbing cells, originate from hematopoietic stem cells. They express high amounts of TRACP-5b and secrete it

into the blood circulation. As reported, TRACP-5b has been used as a marker of bone resorption [39]. In our study, DOP rats showed decreased OCN and BAP and increased TRACP-5b serum levels, which was consistent with previous studies [40, 41]. Reportedly, EB can stimulate osteogenic differentiation of MC3T3-E1 cells [42]. Notably, EB (10 and 20 mg/kg) markedly improved these changes. Bone marrow consists of multiple cell types such as adipocytes, osteoblasts, osteoclasts, stromal cells, and vascular cells. The interaction of these cells maintains a complex homeostatic system for remodeling and regeneration in bone microenvironment [43]. Excessive accumulation of bone marrow adipocytes occurs in diverse clinical conditions, including diabetes, obesity, menopause, aging, anorexia nervosa, glucocorticoid treatment, and radiotherapy, most of which are concomitant with bone deterioration [44]. Expansion of marrow adipose tissue may exaggerate the detrimental bone microenvironment and worsen disease progression [45]. Hematoxylin and eosin staining revealed that EB treatment greatly reduced bone marrow adipocyte density in DOP rats. Bone remodeling is the physiological process by bone mass is maintained. Bone parameters including BMD, BV/TV, Tb.Sp, and Tb.N as well as femur conditions including bone maximum load were evaluated in this study, and we found that EB effectively improved

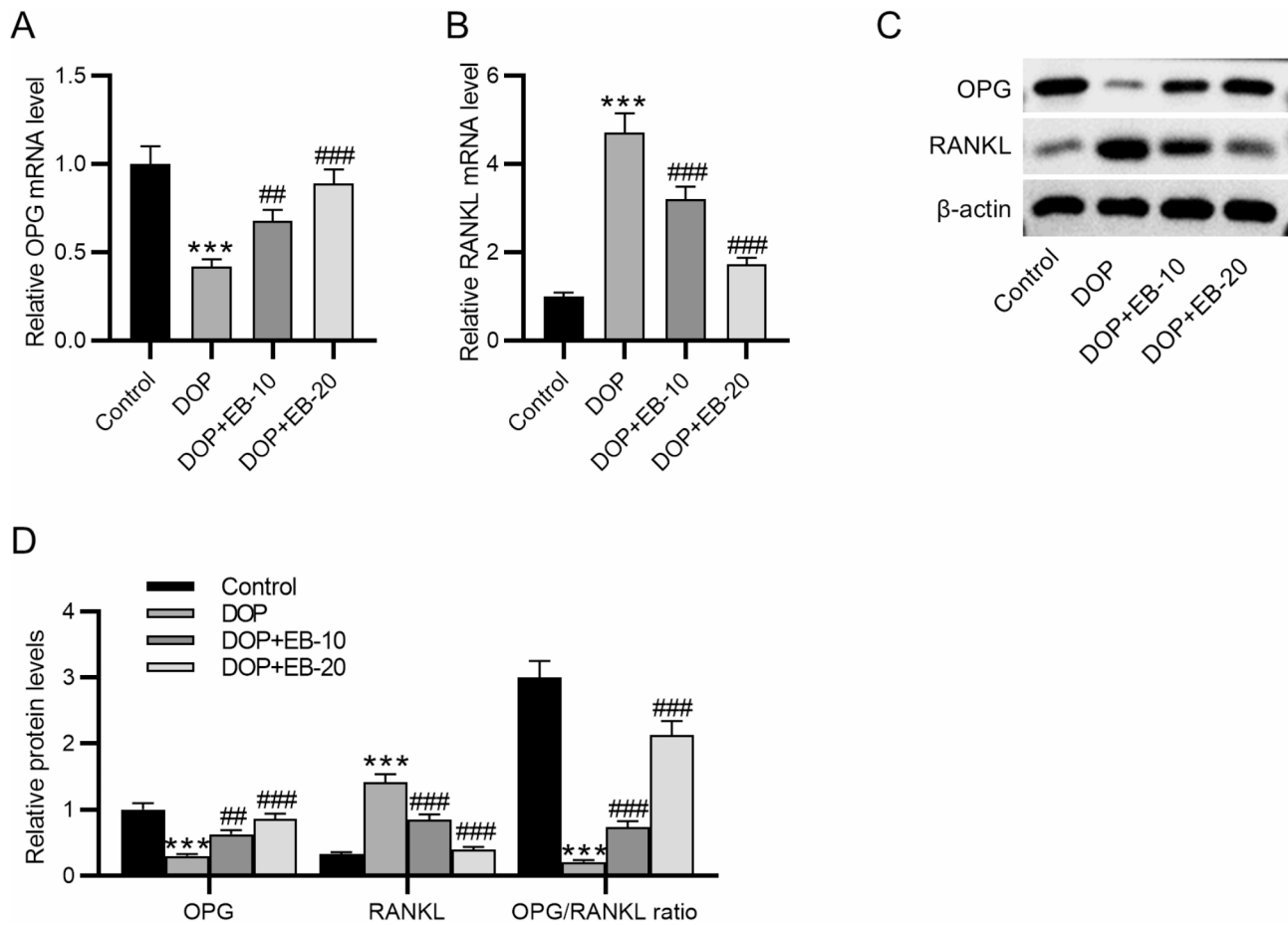


Fig. 5 EB targets the RANKL/OPG axis in DOP rats. **(A)** RT-qPCR of OPG mRNA level in rat femur. **(B)** RT-qPCR of RANKL mRNA level in rat femur. **(C)** Representative images of OPG and RANKL protein bands. **(D)** Relative protein levels of OPG and RANKL normalized to β -actin. *** $p < 0.001$ vs. Control group; ## $p < 0.01$, ### $p < 0.001$ vs. DOP group

bone mass loss, in consistent with previous findings [23]. These findings suggest that EB effectively promotes bone formation and inhibits bone resorption and bone marrow adipogenesis in DOP rats, indicating its potential in DOP treatment.

Hyperglycemia, a condition that occurs when blood glucose levels are too high, is a common complication of diabetes. Hyperglycemia can trigger metabolic pathways that lead to inflammation, cytokine secretion, cell death, and consequently diabetic complications [46]. Inflammation is a major cause of bone homeostasis imbalance [47]. The anti-inflammatory effect of EB has been previously documented. EB significantly inhibits acute inflammation and ameliorates the neuroinflammation-associated impairment of locomotion in a zebrafish inflammation model induced by copper sulfate and tail cutting by inactivating the MAPK/NF- κ B/Nod-like receptor pathways [27]. In this study, our data revealed that EB administration greatly reversed the STZ-induced increases in serum levels of inflammatory factors such as TNF- α , IL-6, and

MCP-1, indicating that EB may inhibit inflammation in DOP rats.

In the process of osteoclast differentiation and activation, osteoblasts express RANKL and OPG. OPG, also known as osteoclastogenesis inhibitory factor, is produced by osteoblasts and osteogenic stromal stem cells. OPG protects against excessive bone resorption by binding to RANKL and prevents it from interacting with RANK [48]. Compared to controls, diabetic patients exhibit lower plasma OPG level and higher serum RANKL level [49], and the significantly higher RANKL/OPG ratio in diabetic patients indicates increased differentiation and activation and enhanced bone resorption, leading to osteoporosis [50]. Additionally, hyperglycemia and inflammation caused by diabetes might lead to an increased RANKL/OPG ratio and result in excessive bone resorption, ultimately increasing the fracture risk [51–53]. The concentration of OPG and RANKL for osteoclast differentiation is regulated by lysosomal cytokines, such as TNF- α and IL-6, which stimulate osteoclastogenesis by reducing OPG ligand expression [26].

Our results revealed that EB treatment increased OPG and decreased RANKL mRNA and protein levels and enhanced the OPG/RANKL ratio in DOP rats, indicating that EB may maintain bone homeostasis by regulating the OPG/RANKL pathway.

There are limitations to this study. First, there is no detailed pharmacokinetic analysis of EB, which is essential for understanding its absorption, distribution, metabolism, and excretion. Second, while the study indicates that EB acts through the OPG/RANKL pathway, it may not fully rule out or distinguish other potential off-target effects of pathways that could contribute to the observed outcomes. Third, EB was administered intragastrically; other potentially more effective routes, such as intravenous or intrathecal, were not explored. Fourth, this study did not test EB on human cell lines or primary cultures, which can help validate the findings from rodent models. These limitations will be addressed in the future.

Conclusion

In conclusion, this study demonstrates that EB supplementation could attenuate STZ-induced DOP in rats by promoting bone formation and inhibiting bone resorption and inflammation through upregulating the OPG/RANKL ratio. This study might promote the clinical application of EB in preventing and treating DOP.

Supplementary Information

The online version contains supplementary material available at <https://doi.org/10.1186/s13018-025-05685-4>.

Supplementary Material 1

Acknowledgements

The authors appreciate the help of Wuhan Third Hospital.

Author contributions

Xianmei Zhang conceived and designed the experiments. Xianmei Zhang, Qinguo Sun, Xie Xie, Meng Luo, Junjie Zan and Zewei Cong carried out the experiments. Xianmei Zhang, Qinguo Sun, Xie Xie, Meng Luo, Junjie Zan and Zewei Cong analyzed the data. Xianmei Zhang and Zewei Cong drafted the manuscript. All authors agreed to be accountable for all aspects of the work. All authors have read and approved the final manuscript.

Funding

The work was supported by Wuhan Municipal and Health Research Fund (Study on the Mechanism of Ziyin Bushen Formula Regulating Intestinal Flora to Improve Diabetic Osteoporosis, WZ24B39).

Data availability

The datasets used or analyzed during the current study are available from the corresponding author on reasonable request.

Declarations

Ethical approval

All animal experiments were reviewed and approved by Wuhan Myhalic Biotechnology Co., Ltd (approval number: HLK-202309244; approval date: September 15, 2023).

Disclosure

No.

Competing interests

The authors declare no competing interests.

Received: 26 November 2024 / Accepted: 4 March 2025

Published online: 22 April 2025

References

1. Sun H, Saeedi P, Karuranga S, Pinkepank M, Ogurtsova K, Duncan BB, et al. IDF diabetes atlas: global, regional and country-level diabetes prevalence estimates for 2021 and projections for 2045. *Diabetes Res Clin Pract*. 2022;183:109119.
2. Paschou SA, Dede AD, Anagnostis PG, Vryonidou A, Morganstein D, Goulis DG. Type 2 diabetes and osteoporosis: A guide to optimal management. *J Clin Endocrinol Metab*. 2017;102(10):3621–34.
3. Lin HH, Hsu HY, Tsai MC, Hsu LY, Chien KL, Yeh TL. Association between type 2 diabetes and osteoporosis risk: A representative cohort study in Taiwan. *PLoS ONE*. 2021;16(7):e0254451.
4. Liu X, Chen F, Liu L, Zhang Q. Prevalence of osteoporosis in patients with diabetes mellitus: a systematic review and meta-analysis of observational studies. *BMC Endocr Disord*. 2023;23(1):1.
5. Li T, Hu L, Yin XL, Zou Y, Fu HY, Li HL. Prevalence and risk factors of osteoporosis in patients with type 2 diabetes mellitus in Nanchang (China): A retrospective cohort study. *Diabetes Metab Syndr Obes*. 2022;15:3039–48.
6. Migliorini F, Colarossi G, Eschweiler J, Oliva F, Driessen A, Maffulli N. Anti-resorptive treatments for corticosteroid-induced osteoporosis: a bayesian network meta-analysis. *Br Med Bull*. 2022;143(1):46–56.
7. Conti V, Russomanno G, Corbi G, Toro G, Simeon V, Filippelli W, et al. A polymorphism at the translation start site of the vitamin D receptor gene is associated with the response to anti-osteoporotic therapy in postmenopausal women from Southern Italy. *Int J Mol Sci*. 2015;16(3):5452–66.
8. Migliorini F, Maffulli N, Colarossi G, Eschweiler J, Tingart M, Betsch M. Effect of drugs on bone mineral density in postmenopausal osteoporosis: a bayesian network meta-analysis. *J Orthop Surg Res*. 2021;16(1):533.
9. Mohsin S, Baniyas MM, AIDarmaki RS, Tekes K, Kalász H, Adeghate EA. An update on therapies for the treatment of diabetes-induced osteoporosis. *Expert Opin Biol Ther*. 2019;19(9):937–48.
10. Khosla S, Hofbauer LC. Osteoporosis treatment: recent developments and ongoing challenges. *Lancet Diabetes Endocrinol*. 2017;5(11):898–907.
11. Bolamperti S, Villa I, Rubinacci A. Bone remodeling: an operational process ensuring survival and bone mechanical competence. *Bone Res*. 2022;10(1):48.
12. Brown C. Staying strong. *Nature*. 2017;550(7674):S15–7.
13. Orimo H. The mechanism of mineralization and the role of alkaline phosphatase in health and disease. *J Nippon Med Sch*. 2010;77(1):4–12.
14. Licini C, Vitale-Brovarone C, Mattioli-Belmonte M. Collagen and non-collagenous proteins molecular crosstalk in the pathophysiology of osteoporosis. *Cytokine Growth Factor Rev*. 2019;49:59–69.
15. Udagawa N, Takahashi N, Yasuda H, Mizuno A, Itoh K, Ueno Y, et al. Osteoprotegerin produced by osteoblasts is an important regulator in osteoclast development and function. *Endocrinology*. 2000;141(9):3478–84.
16. Cao G, Hu S, Ning Y, Dou X, Ding C, Wang L, et al. Traditional Chinese medicine in osteoporosis: from pathogenesis to potential activity. *Front Pharmacol*. 2024;15:1370900.
17. Song F, Wei C, Zhou L, Qin A, Yang M, Tickner J, et al. Luteoloside prevents lipopolysaccharide-induced osteolysis and suppresses RANKL-induced osteoclastogenesis through attenuating RANKL signaling cascades. *J Cell Physiol*. 2018;233(2):1723–35.
18. Lee JW, Kobayashi Y, Nakamichi Y, Udagawa N, Takahashi N, Im NK, et al. Alisol-B, a novel phyto-steroid, suppresses the RANKL-induced osteoclast formation and prevents bone loss in mice. *Biochem Pharmacol*. 2010;80(3):352–61.
19. Wang T, Liu Q, Zhou L, Yuan JB, Lin X, Zeng R, et al. Andrographolide inhibits Ovariectomy-Induced bone loss via the suppression of RANKL signaling pathways. *Int J Mol Sci*. 2015;16(11):27470–81.
20. Choi SW, Park KI, Yeon JT, Ryu BJ, Kim KJ, Kim SH. Anti-osteoclastogenic activity of Matairesinol via suppression of p38/ERK-NFATc1 signaling axis. *BMC Complement Altern Med*. 2014;14:35.

21. Satué M, Arriero Mdel M, Monjo M, Ramis JM. Quercitrin and taxifolin stimulate osteoblast differentiation in MC3T3-E1 cells and inhibit osteoclastogenesis in RAW 264.7 cells. *Biochem Pharmacol*. 2013;86(10):1476–86.
22. Sze SC, Tong Y, Ng TB, Cheng CL, Cheung HP. Herba epimedii: anti-oxidative properties and its medical implications. *Molecules*. 2010;15(11):7861–70.
23. Diao X, Wang L, Zhou Y, Bi Y, Zhou K, Song L. The mechanism of Epimedin B in treating osteoporosis as revealed by RNA sequencing-based analysis. *Basic Clin Pharmacol Toxicol*. 2021;129(6):450–61.
24. Garcia C, Feve B, Ferré P, Halimi S, Baizri H, Bordier L, et al. Diabetes and inflammation: fundamental aspects and clinical implications. *Diabetes Metab*. 2010;36(5):327–38.
25. Jiao H, Xiao E, Graves DT. Diabetes and its effect on bone and fracture healing. *Curr Osteoporos Rep*. 2015;13(5):327–35.
26. Weitzmann MN. The role of inflammatory cytokines, the RANKL/OPG axis, and the immunoskeletal interface in physiological bone turnover and osteoporosis. *Scientifica (Cairo)*. 2013;2013:p125705.
27. Liu L, Zhong Y, Zheng T, Zhao J, Ding S, Lv J, et al. Epimedin B exerts an anti-inflammatory effect by regulating the MAPK/NF- κ B/NOD-like receptor signalling pathways. *Fish Shellfish Immunol*. 2024;150:109657.
28. Gheibi S, Kashfi K, Ghasemi A. A practical guide for induction of type-2 diabetes in rat: incorporating a high-fat diet and streptozotocin. *Biomed Pharmacother*. 2017;95:605–13.
29. Liu S, Liu Q, Peng Q, Zhang Y, Wang J. [Dihydromyricetin improves cardiac insufficiency by inhibiting HMGB1 in diabetic rats]. *Nan Fang Yi Ke Da Xue Xue Bao*. 2022;42(5):641–8.
30. Zhang M, Hu ZF, Dong XL, Chen WF. Epimedin B exerts neuroprotective effect against MPTP-induced mouse model of Parkinson's disease: GPER as a potential target. *Biomed Pharmacother*. 2022;156:113955.
31. Rieger R, Auregan JC, Hoc T. Micro-finite-element method to assess elastic properties of trabecular bone at micro- and macroscopic level. *Morphologie*. 2018;102(336):12–20.
32. Xu Y, Wu Q. Trends in osteoporosis and mean bone density among type 2 diabetes patients in the US from 2005 to 2014. *Sci Rep*. 2021;11(1):3693.
33. Shah VN, Harrall KK, Shah CS, Gallo TL, Joshee P, Snell-Bergeon JK, et al. Bone mineral density at femoral neck and lumbar spine in adults with type 1 diabetes: a meta-analysis and review of the literature. *Osteoporos Int*. 2017;28(9):2601–10.
34. Ma L, Oei L, Jiang L, Estrada K, Chen H, Wang Z, et al. Association between bone mineral density and type 2 diabetes mellitus: a meta-analysis of observational studies. *Eur J Epidemiol*. 2012;27(5):319–32.
35. Lee JH, Jin H, Shim HE, Kim HN, Ha H, Lee ZH. Epigallocatechin-3-gallate inhibits osteoclastogenesis by down-regulating c-Fos expression and suppressing the nuclear factor- κ B signal. *Mol Pharmacol*. 2010;77(1):17–25.
36. Zhang ND, Han T, Huang BK, Rahman K, Jiang YP, Xu HT, et al. Traditional Chinese medicine formulas for the treatment of osteoporosis: implication for antiosteoporotic drug discovery. *J Ethnopharmacol*. 2016;189:61–80.
37. Wang L, Li Y, Guo Y, Ma R, Fu M, Niu J, et al. Herba epimedii: an ancient Chinese herbal medicine in the prevention and treatment of osteoporosis. *Curr Pharm Des*. 2016;22(3):328–49.
38. Noh JY, Yang Y, Jung H. Molecular mechanisms and emerging therapeutics for osteoporosis. *Int J Mol Sci*. 2020. 21(20).
39. Lv Y, Wang G, Xu W, Tao P, Lv X, Wang Y. Tartrate-resistant acid phosphatase 5b is a marker of osteoclast number and volume in RAW 264.7 cells treated with receptor-activated nuclear KB ligand. *Exp Ther Med*. 2015;9(1):143–6.
40. Guo CJ, Xie JJ, Hong RH, Pan HS, Zhang FG, Liang YM. Puerarin alleviates streptozotocin (STZ)-induced osteoporosis in rats through suppressing inflammation and apoptosis via HDAC1/HDAC3 signaling. *Biomed Pharmacother*. 2019;115:108570.
41. Xie H, Wang Q, Zhang X, Wang T, Hu W, Manicum T, et al. Possible therapeutic potential of Berberine in the treatment of STZ plus HFD-induced diabetic osteoporosis. *Biomed Pharmacother*. 2018;108:280–7.
42. Guo Y, Wang X, Gao J. Simultaneous Preparation and comparison of the osteogenic effects of Epimedin A - C and Icarin from Epimedium Brevicornu. *Chem Biodivers*. 2018;15(4):e1700578.
43. Ambrosi TH, Scialdone A, Graja A, Gohlke S, Jank AM, Bocian C, et al. Adipocyte accumulation in the bone marrow during obesity and aging impairs stem Cell-Based hematopoietic and bone regeneration. *Cell Stem Cell*. 2017;20(6):771–e7846.
44. Sebo ZL, Rendina-Ruedy E, Ables GP, Lindskog DM, Rodeheffer MS, Fazeli PK, et al. Bone marrow adiposity: basic and clinical implications. *Endocr Rev*. 2019;40(5):1187–206.
45. Bukowska J, Frazier T, Smith S, Brown T, Bender R, McCarthy M, et al. Bone marrow adipocyte developmental origin and biology. *Curr Osteoporos Rep*. 2018;16(3):312–9.
46. Volpe CMO, Villar-Delfino PH, Dos PMF, Anjos JA, Nogueira-Machado. Cellular death, reactive oxygen species (ROS) and diabetic complications. *Cell Death Dis*. 2018;9(2):119.
47. Lee EJ, Song DH, Kim YJ, Choi B, Chung YH, Kim SM, et al. PTX3 stimulates osteoclastogenesis by increasing osteoblast RANKL production. *J Cell Physiol*. 2014;229(11):1744–52.
48. Boyce BF, Xing L. The RANKL/RANK/OPG pathway. *Curr Osteoporos Rep*. 2007;5(3):98–104.
49. Karalazou P, Ntelios D, Chatzopoulou F, Fragou A, Taousani M, Mouzaki K, et al. OPG/RANK/RANKL signaling axis in patients with type I diabetes: associations with parathormone and vitamin D. *Ital J Pediatr*. 2019;45(1):161.
50. Yasuda H. RANKL, a necessary chance for clinical application to osteoporosis and cancer-related bone diseases. *World J Orthop*. 2013;4(4):207–17.
51. Mitama Y, Fujiwara S, Yoneda M, Kira S, Kohno N. Association of type 2 diabetes and an inflammatory marker with incident bone fracture among a Japanese cohort. *J Diabetes Investig*. 2017;8(5):709–15.
52. Iqbal J, Yuen T, Sun L, Zaidi M. From the gut to the strut: where inflammation reigns, bone abstains. *J Clin Invest*. 2016;126(6):2045–8.
53. Lei C, Xueming H, Ruihang D. MLN64 deletion suppresses RANKL-induced osteoclastic differentiation and attenuates diabetic osteoporosis in streptozotocin (STZ)-induced mice. *Biochem Biophys Res Commun*. 2018;505(4):1228–35.

Publisher's note

Springer Nature remains neutral with regard to jurisdictional claims in published maps and institutional affiliations.